substituted polyesters having lower t_{KN} values must have smaller chain extensions at ambient temperatures. The poor mechanical properties reported by Acierno et al.[4] for fibers spun from the nematic phases of semiflexible polyesters would lead us to expect, therefore, that the more flexible H/C_6H_5 would have poorer fiber properties than C_6H_5/H. This does appear to be the case. The Harris patent[10] cites for heat-treated fibers of H/C_6H_5 the following values for the tenacity, (g/denier), elongation (%), and modulus (g/denier): 10.0/3.14/352. Jackson[6] gave for a heat-treated fiber of C_6H_5/H the values 32/4.3/910.

Acknowledgment. This work was supported by the U.S. Army Research Office on Contract DAAG29-84-0033.

References and Notes

(1) Acierno, D.; La Mantia, F. P.; Polizzotti, G.; Ciferri, A.; Krigbaum, W. R.; Kotek, R. *J. Polym. Sci., Polym. Phys. Ed.* **1983**, *21*, 2027.
(2) Arpin, M.; Strazielle, G. *Polymer* **1977**, *18*, 591.
(3) Erman, B.; Flory, P. J.; Hummel, J. P. *Macromolecules* **1980**, *13*, 484.
(4) Krigbaum, W. R.; Ciferri, A. *J. Polym. Sci., Polym. Lett. Ed.* **1980**, *15*, 253.
(5) Frosini, V.; Levita, G.; Landis, J.; Woodward, A. E. *J. Polym. Sci., Polym. Phys. Ed.* **1977**, *15*, 239.
(6) Jackson, W. J., Jr. *Br. Polym. J.* **1980**, *12*, 154.
(7) Economy, J.; Storm, R. S.; Matkovich, V. I.; Cottis, S. G.; Nowak, B. E. *J. Polym. Sci., Polym. Chem. Ed.* **1976**, *14*, 2207.
(8) Goodman, I.; McIntyre, J. E.; Aldred, D. H. British Patent 993 272, 1975.
(9) Payet, C. R. U.S. Patent 4 159 365, 1979.
(10) Harris, J. F.; Jr. U.S. Patent 4 294 955, 1981.
(11) Majnusz, J.; Catala, J. M.; Lenz, R. W. *Eur. Polym. J.* **1983**, *19*, 1043.
(12) Dicke, H.-R.; Lenz, R. W. *J. Polym. Sci., Polym. Chem. Ed.* **1983**, *21*, 2581.
(13) Cottes, S. G.; Economy, J.; Nowak, B. E. U.S. Patent 3 637 595, 1972.
(14) Schaefgen, J. R. U.S. Patent 4 118 372, 1978.
(15) Calundann, G. W. U.S. Patent 4 184 996, 1980.
(16) Irwin, R. S. U.S. Patent 4 335 232, 1982.
(17) Favstritsky, N. A. U.S. Patent 4 337 191, 1982.
(18) Kleinschuster, J. J.; Pletcher, T. C.; Schaefgen, J. R. Belgian Patent 828 935, 1975.
(19) Jin, J.-I.; Antoun, S.; Ober, C.; Lenz, R. W. *Br. Polym. J.* **1980**, *12*, 132.
(20) Kuhfuss, H. F.; Jackson, W. J., Jr. U.S. Patent 3 778 410, 1973.
(21) Weissberger, E. K.; Weissberger, J. H. *J. Org. Chem.* **1958**, *23*, 1193.
(22) Love, J. L.; Peak, D. A.; Watkins, T. I. *J. Chem. Soc.* **1951**, 3286.
(23) Hawthorne, M. F.; Reintjes, M. *J. Am. Chem. Soc.* **1965**, *87*, 4585.
(24) Ringsdorf, A.; Schmidt, H. W.; Schneller, A. *Makromol. Chem., Rapid Commun.* **1982**, *3*, 745.
(25) Casgrande, C.; Veyssie, M.; Finkelmann, H. F. *J. Phys. (Paris)* **1982**, *43*, L671.
(26) Sackmann, H.; Demus, D. *Mol. Cryst.* **1982**, *2*, 81.
(27) Sackmann, H.; Demus, D. *Mol. Cryst. Liq Cryst.* **1973**, *21*, 239.
(28) Watanabe, J.; Krigbaum, W. R. *Macromolecules* **1984**, *17*, 2288.
(29) Luise, R. R. U.S. Patent 4 183 895, 1980.
(30) Kyotani, M.; Kanetsuna, H. *J. Polym. Sci., Polym. Phys. Ed.* **1983**, *21*, 379.
(31) Flory, P. J.; Ronca, G. *Mol. Cryst. Liq. Cryst.* **1979**, *54*, 311.
(32) Flory, P. J. *Macromolecules* **1978**, *14*, 954.
(33) Krigbaum, W. R.; Hakemi, H.; Ciferri, A.; Conio, G. *Macromolecules*, following article in this issue.

Comparison of the Phase Behavior of Binary Systems Involving Low and High Molecular Weight Thermotropic Nematogens

W. R. Krigbaum,* H. Hakemi,† A. Ciferri,‡ and G. Conio§

Department of Chemistry, Duke University, Durham, North Carolina 27706.
Received August 30, 1984

ABSTRACT: Binary phase diagrams were determined for the low molecular weight nematogen *p*-azoxyanisole with diluents *N,N*-diphenylacetamide and acetanilide. Comparison with the Warner–Flory theory indicates the width of the biphasic region is correctly estimated, but the predicted depression of T_{NI} is too large. Moreover, the two diluents give different depressions, suggesting a dependence of the nematic order upon the shape of the diluent molecule. The observed depressions of T_{KN} are also compared with prediction. The isotropization temperatures were determined for poly(*n*-hexyl isocyanate) (PHIC) in toluene, and the temperature dependence of the persistence length of PHIC was determined from viscosity data in toluene and tetrahydrofuran (THF). The nematic range of PHIC extends over a very broad composition range, which cannot be accounted for in terms of hard and soft interactions. Flory's treatment of Kuhn chain polymers is modified to account for the temperature dependence of the unperturbed dimensions. For PHIC, extrapolation of the axial ratio of the Kuhn link to $T_{NI}°$ follows expectation. For other polymers, such as (hydroxypropyl)cellulose, a small contribution from soft interactions may be necessary. We suggest that a negative temperature coefficient plays an important role in the mesophase behavior of rigid-chain polymers, and perhaps even of low molecular weight nematogens.

Introduction

Early statistical mechanical treatments of nematic phenomena stressed the effect of the asymmetric shape of the nematogen upon the entropy of the system. Both the virial aproach of Onsager[1] and Ishihara[2] and the lattice model treatment of Flory[3] demonstrated that a solution of rodlike particles will transform to an anisotropic nematic phase when the concentration of rods exceeds a critical value which is dependent upon the axial ratio of the rod. By contrast, the theory of Maier and Saupe[4] postulated that the nematic phase is stabilized solely by energy difference arising from orientation-dependent interactions. Their treatment was concerned with thermotropic mesomorphism in one-component systems. It is now recognized that the nematic phase may be stabilized by both energy and entropy differences between the nematic and isotropic phases. Both effects were incorporated in a treatment of

† Present address: Physical Research, B.C. Johnson and Son, Inc., Racine, WI 53403.
‡ Istituto Chimica Industriale, University of Genoa, Genoa, Italy.
§ Centro Macromolecole CNR, University of Genoa, Genoa, Italy.

0024-9297/85/2218-0973$01.50/0

one-component rodlike nematogens by Flory and Ronca.[5] An important conclusion of their work is that a thermotropic nematic–isotropic transition will only be observed if the axial ratio of the nematogen is less than a critical value, 6.417. If the axial ratio exceeds the critical value, the entropy difference is sufficient to stabilize the nematic phase, and only lyotropic mesomorphism should be observed. An extension of this treatment due to Warner and Flory[6] accounts for the diminution of orientation-dependent interactions when a spherical diluent is added to a rodlike nematogen. Hence, this treatment affords predictions for binary systems composed of a low molecular weight nematogen and a diluent.

In seeking an appropriate experimental system for comparison with the prediction of their theory, Flory and Ronca[5] placed special emphasis upon the requirements that the nematogen be rigid and rodlike and have approximate cylindrical symmetry. This led them to propose the *p*-phenylene oligomers as suitable nematogens. This system has since been extensively studied,[7-10] but the high transition temperatures and poor solubility make experimental investigation difficult. One can anticipate[11] that these experimental problems will be a common feature of the nematogens which fulfill the criteria set forth by Flory and Ronca. Binary systems should offer a more facile route for comparison of experiment with theory.

The investigation of binary nematogenic systems has had a very long history, dating almost from the beginning of liquid crystal research. For example, in 1904 de Kock[12] reported complete phase diagrams for systems comprised of *p*-azoxyanisole and various diluents. He made a number of significant observations in this early work. de Kock found that the addition of a small amount of diluent creates a biphasic region in which the nematic and isotropic phases coexist and that the biphasic temeperatures decrease in an approximately linear fashion with increasing diluent concentration. Since no statistical treatment of the nematic phase was available, he analyzed his data by applying an earlier theory of Rothmund[13] for the depression of the melting temperature of a mixed crystal. The result obtained, upon assuming that the nematogenic component obeys Raoult's law in both phases, is

$$x_1 - x_1' = \frac{\Delta S_{NI}}{R}\left(\frac{T_{NI}^\circ - T_{NI}}{T_{NI}^\circ}\right) \qquad (1)$$

where x_1 and x_1' are the mole fractions of diluent in the isotropic and nematic phases, ΔS_{NI} is the entropy change at the nematic–isotropic transition, R is the gas constant, and T_{NI} and T_{NI}° are the nematic–isotropic transition temperatures of the binary system and the pure nematogen, respectively. Of course, this relation does not allow prediction of the biphasic temperatures for a particular diluent concentration. However, by fitting data for the mixture of hydroquinone and *p*-azoxyanisole, de Kock obtained a reasonable value for the enthalpy change at the nematic–isotropic transition, $\Delta H_{NI} = 175$ cal/mol. Martire and co-workers,[14,15] in a thermodynamic treatment of the equilibrium between two phases, obtained a relation which reduced to eq 1 after some approximations.

Earlier attempts to predict the phase diagram of binary nematogenic systems have often involved assumptions which are clearly incorrect. For example, Kronberg and Patterson[16] assumed that the Flory–Huggins chemical potentials could be used for components in the nematic phase. They rationalized this usage on the grounds that the treatment applies equally well to rods and coiling molecules. Although this statement is true, the derivation of the Flory–Huggins entropy implicitly assumes an isotropic phase, so that it cannot be applied to a highly ordered nematic phase. This was demonstrated much earlier by Flory's lattice model treatment of semiflexible molecules.[17] Cox and Johnson[18] concluded that, because a solid melts to either a nematic or isotropic phase by a first-order transition, both melting depressions must obey the same type of thermodynamic relationship. Martire and his coworkers[19-22] treated a number of different cases using a lattice model, but adopted the DiMarzio[23] approach in which the rods are restricted to three mutually perpendicular directions.

The treatment of binary systems by Warner and Flory[6] avoids these objections. As indicated above, binary systems offer an easier route for the comparison of experiment with theory. Hence, to provide a test of the predictions of the Warner–Flory treatment, we have collected data for *p*-azoxyanisole in two diluents, *N*,*N*-diphenylacetamide and acetanilide.

Turning to polymeric nematogens, theoretical treatment of their behavior is in a more rudimentary state. Flory,[24,25] in his treatment of Kuhn chain polymers, observed that the nematogenic behavior is governed by the axial ratio of the Kuhn link and that the contour length of the chain has little effect upon their mesogenic properties. This suggests that the Warner–Flory treatment could be applied to predict the thermotropic behavior of binary systems involving polymeric nematogens if the polymer behaves as a Kuhn chain, and if the dimensions of the Kuhn link are known from independent measurements.

As noted above, the Flory–Ronca treatment[5] predicts that there is a critical axial ratio above which the nematic–isotropic transition temperature, T_{NI}°, becomes infinite. The axial ratio is assumed to be independent of temperature in these treatments. However, it is well recognized[26] that the unperturbed dimensions of coiling macromolecules are temperature dependent. The coefficient is generally negative for molecules with relatively highly extended chains. This fact suggests an alternative mechanism for a thermotropic nematic–isotropic transition in polymers. Even if the axial ratio exceeds the critical value at a particular temperature, T_{NI}° cannot be infinite because at some higher temperature the axial ratio will decrease to the critical value, and T_{NI}° must coincide with this temperature. We will introduce these considerations in the treatment by Flory of Kuhn chain polymers (which does not involve soft interactions) and test the proposed mechanism with experimental data for poly(*n*-hexyl isocyanate) and with literature data for (hydroxypropyl)cellulose (HPC).

Experimental Section

***p*-Azoxyanisole.** *N*,*N*-diphenylacetamide (DPA) and acetanilide (AA) were obtained from Eastman Chemical Co., and *p*-azoxyanisole (PAA) was purchased from Aldrich Chemicals. PAA and AA were recrystallized from benzene, and DPA was crystallized from a mixture of water and ethanol. The crystalline products were dried overnight in a vacuum oven at 80 °C. Characteristics of these compounds are collected in Table I.

Mixtures were prepared by direct weighing into high-pressure differential scanning calorimeter pans. The powders were thoroughly mixed and the pan was sealed and heated for 5 min at a temperature just within the isotropic region to achieve complete mixing. The phase transition were observed by using an Olympus BH-2 polarizing microscope equipped with a Mettler FP52 hot stage and FP5 temperature controller. The heating rate was typically 1 °C/min and the transition temperatures as measured by microscope were generally reproducible to within ±0.2 °C, and those by DSC to within ±0.5 °C. Photomicrographs were taken by using a Nikon polaroid camera attachment. The transition enthalpies were determined by using a Du Pont 910 differential scanning calorimeter with a 1090 analyzer. Transition

Table I
Physical and Thermal Properties of PAA and Diluents

compd	mol wt	density, g/cm³	transition temp, K	ΔH_{KN} (ΔH_{KI}), kcal/mol	ΔH_{NI}, kcal/mol	ΔS_{KN} (ΔS_{KI}), cal/(mol K)	ΔS_{NI}, cal/(mol K)
p-azoxyanisole	258.3	1.148,[a] 1.343[b]	KIII(389.6)N(408.3)I	6.67	0.158	17.1	0.387
N,N-diphenylacetamide	211.3	1.135,[a] 1.225[b]	K(373.1)I	(5.29)		(14.7)	
acetanilide	135.2	1.014[a]	K(386.7)I	(5.09)		(16.2)	

[a] Density at 133 °C. [b] Density at 25 °C.

temperatures for the PAA systems were read from the leading edge of the exotherm or endotherm.

Poly(*n*-hexyl isocyanate). Of the 10 poly(*n*-hexyl isocyanate) (PHIC) samples used, six are identical with those studied previously[27] and an additional four were obtained by fractionating sample AI. Molecular weights were determined from the intrinsic viscosities in toluene at 25 °C by using the relation of Berger and Tidswell,[28] $[\eta] = 2.48 \times 10^{-5} M^{1.05}$. The technique previously described[27] was used to determine the persistence length from viscosities in toluene (R. G. Riedel de Haen AG) in the temperature range 25–99 °C (bp 110 °C), and in tetrahydrofuran (THF) stabilized with 2,6-di-*tert*-butyl-4-methylphenol (Riedel de Haan AG) between 12 and 51 °C (bp 65 °C). We also attempted to use tetrachloroethane as a solvent, as reported by Aharoni and Walsh;[29] however, we noticed extensive degradation with this solvent. The thermal expansion of the solvent was accounted for in evaluating the concentration of the solutions at different temperatures. The temperature dependence of the critical concentration, C_p' (g of PHIC/g of solution) was determined by using a Mettler FP-52 hot stage and polarizing microscope to locate the temperature at which the birefringence completely disappears. These measurements were performed for sample KI in toluene by using heating rates of 3 °C/min to within 10 °C of the transition, and 1 °C/min in the transition region. Polymer volume fractions were calculated from C_p by assuming additivity and using the specific volume of the polymer in toluene determined pycnometrically,[27] $\bar{v}_2 = 1.000$ mL/g. The transition temperature, $T_{NI}°$, was also determined for the undiluted polymer as a function of molecular weight.

Results

Binary Systems Involving *p*-Azoxyanisole. In common with many low molecular weight and polymeric nematogens, *p*-azoxyanisole exhibits crystalline polymorphism. Two crystal modifications were examined by Bernal and Crowfoot[30] in their X-ray crystal study reported in 1933. In 1968 Robinder and Poirier[31] obtained evidence for a third crystal polymorph in their study of a recrystallized and zone-refined sample. The phase transitions they reported are indicated in the following diagram (temperatures given in °C):

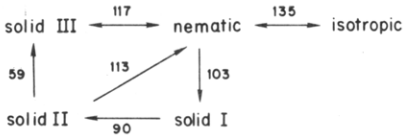

Solid III is the stable form at room temperature, while solid I crystallizes when the nematic phase is cooled. According to Robinder and Poirier, on cooling solid I there is a monotropic transition to solid II which, on further cooling, undergoes a second monotropic transition to solid III. Their evidence for the existence of solid II consisted of a spike in the DSC cooling curve and a solid–nematic transition temperature, 113 °C, which differs from those of the other solid modifications.

Only two solid modifications of PAA had been observed in the earlier calorimetric study by Arnold,[32] and in the DSC investigation of Barrall, Porter, and Johnson.[33] Subsequent work[34-38] has not resolved the question of the number of crystalline polymorphs, nor provided confirming evidence for the existence of the crystal II modification

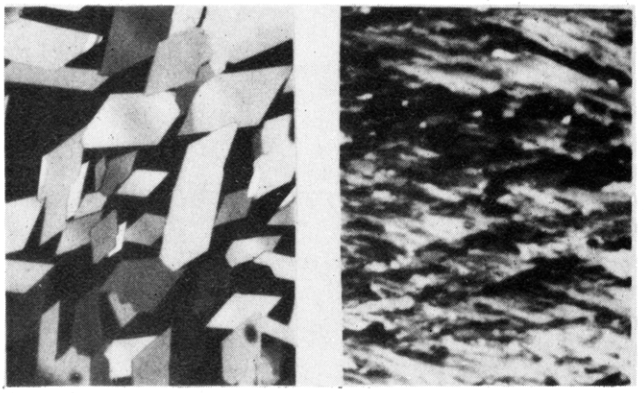

Figure 1. Photomicrographs of two crystalline polymorphs of *p*-azoxyanisole, solid III (left) and solid I (right).

of Robinder and Poirier. These contrasting results emphasize the difficulty in attempting to nucleate a metastable crystal modification in a reproducible manner. Small amounts of adventitious impurities, the interfacial area, and the material of the container may be important factors in this process.

We examined our PAA sample using the hot stage microscope and DSC, but we could find no evidence for the existence of solid II. Cooling the nematic phase produced solid I at 83.9 °C (88 °C by DSC). The nematic phase reappeared upon heating solid I to 104.5 °C (104 °C by DSC). The solid I–solid III transition is kinetically controlled and therefore does not have a transition temperature. In the polarizing microscope the transition was observed to occur rapidly at 59 °C, but it also occurred more slowly at temperatures as high as 92 °C. The solid III–nematic transition was observed at 117.7 °C (117 °C by DSC). Crystals of solid I could be obtained by cooling the nematic phase, but crystalline samples of solid III required seeding. These could be prepared by nearly complete transformation of solid III to the nematic phase at 117 °C, following by slow cooling. The two crystal forms are distinguishable, as illustrated in Figure 1. The two solid modifications could also be observed for the DPA/PAA system when the volume fraction of PAA exceeded 0.92.

Throughout this paper we designate the nematogen as component 2 and the diluent as component 1 and represent the volume fraction of component i by v_i. The complete phase diagram for the DPA/PAA system, based upon the transition temperatures collected in Table II, is shown in Figure 2. The eutectic, representing the equilibrium of the isotropic melt with the crystalline phases of both components, occurs at approximately 355 K and $v_2 = 0.24$. The corresponding phase diagram for the AA/PAA system appears in Figure 3. Data for the latter system, listed in Table III, are more fragmentary and compositions outside the nematic region were mainly studied by using less sensitive instrumentation. The eutectic for the AA/PAA system occurs at approximately 390 K and $v_2 = 0.40$. As expected from the relative magnitudes of the transition enthalpies (Table I), the nematic–biphasic and biphasic–isotropic transition temperatures for both systems are

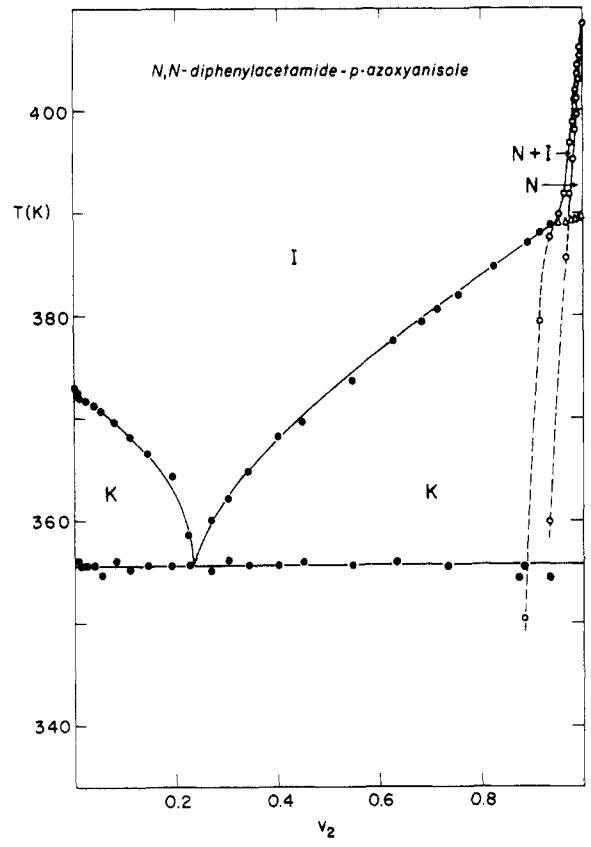

Figure 2. Phase diagram of the system *N,N*-diphenylacetamide/*p*-azoxyanisole.

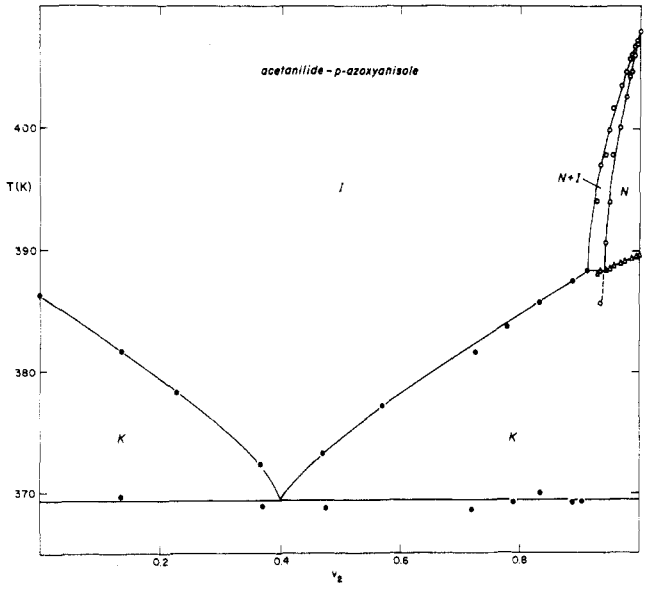

Figure 3. Phase diagram for binary mixtures of acetanilide and *p*-azoxyanisole.

strongly depressed by the addition of diluent, while the depression of the crystal–nematic transition temperature is quite small. As a consequence, the nematic region is confined to a narrow portions of the phase diagram, $v_2 > 0.95$. On cooling the isotropic phase, considerable supercooling is required before crystallization ensues, so that the location of the biphasic region could be traced below the equilibrium melting temperature of the crystalline phase.

Our observations will now be compared with the predictions of the Warner–Flory treatment. For this purpose we introduce a slight modification by replacing their hypothetical standard state (the single-component nematic phase with perfect order) with a standard state having the equilibrium extent of disorder. Let $\mu_2^{\#}$ represent the chemical potential of the nematogen at temperature T in

Table II
Transition Temperatures (K) for *N,N*-Diphenylacetamide and *p*-Azoxyanisole

v_2	v_1	T_{KK}	T_{KI} (T_{KN})	T_N	T_I
1.0000	0.0000		(389.6)		408.2
0.9962	0.0038		(389.5)	405.2	406.1
0.9929	0.0071		(389.5)	402.9	404.7
0.9900	0.0100		(389.3)	401.1	403.5
0.9882	0.0118		(389.1)	399.5	401.9
0.9859	0.0141		(389.3)	398.1	400.8
0.9820	0.0180		(389.2)	395.1	398.9
0.9773	0.0227		(389.1)	391.7	396.8
0.9657	0.0343		(389.1)	385.6	392.9
0.9514	0.0486		(389.3)		390.7
0.9340	0.0660		388.6		387.6
0.9300	0.0700	354.5	389.0	360.0	381.5
0.9169	0.0831		388.0		379.3
0.8929	0.1071		387.1		
0.8800	0.1200	355.5	386.5		350.5
0.8263	0.1737		384.6		
0.7583	0.2417		381.9		
0.7300	0.2700	355.5	381.5		
0.7153	0.2847		380.5		
0.6839	0.3161		379.3		
0.6268	0.3732	356.0	376.5		
0.5465	0.4535	355.6	373.6		
0.4474	0.5526	356.1	369.6		
0.4000	0.6000	355.6	368.1		
0.3422	0.6578	355.6	364.6		
0.3015	0.6985	356.1	362.1		
0.2667	0.7333	355.1	360.1		
0.2267	0.7733	355.6	358.6		
0.1917	0.8083	355.6	364.3		
0.1430	0.8570	355.6	366.6		
0.1100	0.8900	355.1	368.1		
0.0796	0.9204	356.1	369.6		
0.0545	0.9455	354.6	370.0		
0.0399	0.9601	355.6	371.3		
0.0231	0.9769	355.6	371.6		
0.0126	0.9874	355.6	372.1		
0.0068	0.9932	356.1	372.5		
0.0000	1.0000		373.0		

Table III
Transition Temperatures (K) for Acetanilide and *p*-Azoxyanisole

v_2	v_1	T_{KK}	T_{KI} (T_{KN})	T_N	T_I
1.0000	0.0000		(389.7)		408.2
0.9955	0.0045		(389.6)	407.0	407.4
0.9930	0.0070		(389.6)	406.1	407.0
0.9875	0.0125		(389.4)	404.7	406.1
0.9840	0.0160		(389.5)	404.4	405.8
0.9775	0.0225		(389.1)	402.6	404.7
0.9680	0.0320		(388.9)	400.1	403.6
0.9570	0.0430		(388.8)	397.9	401.7
0.9500	0.0500		(388.5)	393.1	399.8
0.9440	0.0560		(388.4)	390.6	397.8
0.9350	0.0650		(388.4)	385.6	397.0
0.9300	0.0700		(388.0)		393.0
0.9200	0.0800		(388.7)		
0.9110	0.0890		388.4		
0.9030	0.0970	379.3	387.1		
0.889	0.111	379.3	387.5		
0.833	0.161	370.0	385.8		
0.779	0.221	369.2	383.8		
0.726	0.274		381.7		
0.570	0.430	368.2	377.2		
0.469	0.531	368.7	373.2		
0.371	0.629	368.9	372.3		
0.2275	0.7725	369.7	378.2		
0.135	0.865	369.7	381.7		
0.000	1.000		386.2		

this standard state, and μ_2° designate that of the same component in the isotropic liquid phase. The change in Gibbs free energy at the nematic–isotropic transition of component 2 can then be written as[5,6]

$$\Delta G_{NI} = \mu_2^\circ - \mu_2^\# = RT^* s_0(1 - s_0/2) - RT(\bar{y}_0 - \zeta - \ln f_1^0) \quad (2)$$

Here ζ is the axial ratio of the rodlike nematogen, T^* is a parameter[5,39] characterizing the strength of the orientation-dependent interactions, s is the order parameter, $\bar{y}$ is the average projection of a rod in the nematic phase upon the plane perpendicular to the preferred direction of the molecules in the nematic phase, and f_1 is the first of several functions (defined below) required to specify the angular distribution of rod orientations in the nematic phase. A subscript or superscript zero has been appended to s, $\bar{y}$, and f_1 to indicate that the values apply to the single-component nematogen.

Since $\Delta G = \Delta H - T\Delta S$, eq 1 yields the following relations for the enthalpy and entropy changes at the nematic–isotropic transition of the single-component system:

$$\Delta H_{NI} = RT^* s_0(1 - s_0/2) \quad (3a)$$

$$\Delta S_{NI} = R(\bar{y}_0 - \zeta - \ln f_1^\circ) \quad (3b)$$

Moreover, since $\Delta G_{NI} = 0$ when the nematogen is at its transition temperature, T_{NI}°

$$\frac{T^*}{T_{NI}^\circ} = \frac{\bar{y}_0 - \zeta - \ln f_1^\circ}{s_0(1 - s_0/2)} \quad (4)$$

This relation, along with those given below for the other parameters involved, can be used to evaluate T^* if T_{NI}° and ζ are known.

For a binary system containing diluent 1, the expressions for the chemical potential differences of the nematogenic component in the nematic phase (designated by a prime) and the isotropic phase are

$$(\mu_2' - \mu_2^\#)/RT = \ln v_2' + v_1' + (v_2'\bar{y} - \bar{y}_0) - \ln (f_1/f_1^0) - (\zeta/\theta)\{(v_2's - s_0) - (1/2)[(v_2's)^2 - s_0^2]\} + \zeta\chi_1 v_1'^2 \quad (5)$$

$$(\mu_2 - \mu_2^\#)/RT = \ln v_2 + v_1 - \bar{y}_0 + \zeta v_2 + \ln f_1^0 + (\zeta/\theta)s_0(1 - s_0/2) + \zeta\chi_1 v_1^2 \quad (6)$$

where θ is the dimensionless ratio T_{NI}/T^* and χ_1 is the customary parameter used to quantify isotropic van der Waals interactions. Setting $\mu_2' = \mu_2$ gives

$$\ln (v_2'/v_2) - (v_2' - v_2) + (v_2'\bar{y} - \zeta v_2) - \ln f_1 - (\zeta/\theta)\{v_2's - (v_2's)^2/2\} + \zeta\chi_1(v_1'^2 - v_1^2) = 0 \quad (7)$$

This is one of the two thermodynamic criteria for the equilibrium between the binary nematic and isotropic phases. It also provides an analogue to eq 4 for the binary system:

$$\zeta/\theta = \zeta T^*/T_{NI}^\circ = \{\ln (v_2'/v_2) - (v_2' - v_2) + (v_2'\bar{y} - \zeta v_2) - \ln f_1 + \zeta\chi_1(v_1'^2 - v_1^2)\}/\{v_2's - (v_2's)^2/2\} \quad (8)$$

The orientation distribution parameters, f_n, are given in terms of integrals over the angle ψ between the rod axis and the preferred direction within the nematic domain:

$$f_n = \int_0^{\pi/2} \exp[-(4\zeta a/\theta)\sin\psi - (3\zeta v_2's/2\theta)\sin^2\psi]\sin^n\psi\, d\psi \quad (9a)$$

where

$$a = -\ln [v_1' + (\bar{y}/\zeta)v_2'] \quad (9b)$$

The parameters $\bar{y}$ and s are expressed in terms of the f_n:[6]

$$\bar{y} = (4\zeta/\pi)(f_2/f_1) \quad (9c)$$

$$s = 1 - (3/2)(f_3/f_1) \quad (9d)$$

The corresponding relations for parameters bearing a subscript or superscript zero are obtained by setting $v_1' = 0$.

The chemical potentials of the diluent in the two phases, taking the isotropic liquid as the standard state, are

$$(\mu_1' - \mu_1^\circ)/RT = \ln v_1' + a + [(\bar{y} - 1)/\zeta]v_2' + (v_2's)^2/2\theta + \chi_1 v_2'^2 \quad (10)$$

$$(\mu_1 - \mu_1^\circ)/RT = \ln v_1 + (1 - 1/\zeta)v_2 + \chi_1 v_2^2 \quad (11)$$

Hence, the second thermodynamic criterion for equilibrium between the binary nematic and isotropic phases, $\mu_1' = \mu_1$, is expressed by

$$\ln (v_1'/v_1) + a + (v_2'\bar{y}/\zeta - v_2) - (v_2' - v_2)/\zeta + (v_2's)^2/2\theta + \chi_1(v_2'^2 - v_2^2) = 0 \quad (12)$$

If desired, one can divide eq 7 by ζ and subtract eq 12 to obtain an alternative relation to be used with either eq 7 or 12:

$$(1/\zeta)\ln (v_2'/v_2) - \ln (v_1'/v_1) - a - (1/\zeta)\ln f_1 - v_2's/\theta - 2\chi_1(v_2' - v_2) = 0 \quad (13)$$

The treatment of nematogenic systems by Flory and co-workers involves the parameters a, s, $\bar{y}$, and the f_n, which are themselves functions of other parameters. Hence, these relations cannot be solved explicitly. Numerical results must be obtained by computer, by using iterative methods to obtain a self-consistent set of parameters which simultaneously satisfy two of the equations (7), (12), and (13). We have used Newton's method to find approximate roots of equations and Simpson's rule to perform numerical integrations.

Transition temperatures measured for the DPA/PAA system at very low diluent concentrations are indicated by the open circles in Figure 4. Within this limited concentration range, the predicted results are essentially independent of χ_1, so we have arbitrarily wet $\chi_1 = 0$. The two full lines in Figure 4 represent the boundaries of the predicted biphasic region using for the axial ratio $\zeta = 3.6$, the value deduced for PAA from structural data by Flory and Ronca.[5] This, in conjunction with $T_{NI}^\circ = 408.3$ given in Table I, yields $T^* = 281$ K, corresponding to $\Delta H_{NI} = 939$ cal/mol. This is nearly 6 times the calorimetric value given in Table I. Comparison with the observed biphasic region indicates that, although the predicted width of the biphasic region is in agreement with the experimental observations, the predicted depressions due to the addition of diluent are too large. If the axial ratio is treated as an adjustable parameter, a reasonable fit (dashed lines) is obtained by using $\zeta = 2.5$. However, T^* is then increased to 520 K, and ΔH_{NI} becomes 1116 cal/mol, or almost 7 times the calorimetric value.

Figure 5 compares the data collected in this concentration range for the AA/PAA and DPA/PAA systems. The Warner–Flory theory treats the diluent as a sphere occupying one lattice site and, as noted above, in this restricted concentration range the term involving χ_1 (isotropic interactions) is inconsequential. Thus, theory predicts that the transition temperature curves for a given nematogen and different diluents should coincide. We find, instead, that the nematic–biphasic and biphasic–isotropic temperatures are depressed less strongly by AA than by DPA. In fact, it was not possible to fit the biphasic region observed for AA/PAA by further reduction of the axial ratio, so the agreement with theory is poorer for

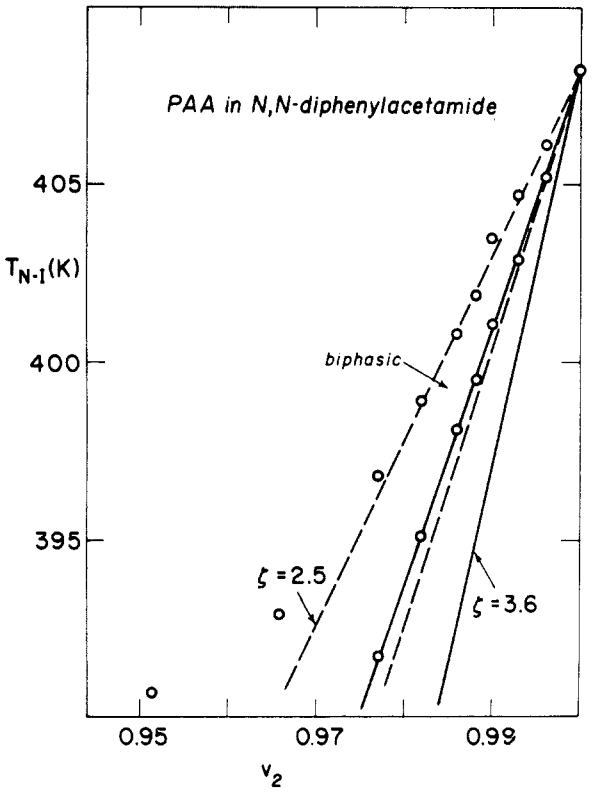

Figure 4. Observed biphasic region for the system diphenylacetamide/*p*-azoxyanisole (circles). Phase boundaries predicted according to the Warner–Flory treatment are shown for axial ratio, ζ, equal to 3.6 (full lines) and 2.5 (dashed lines).

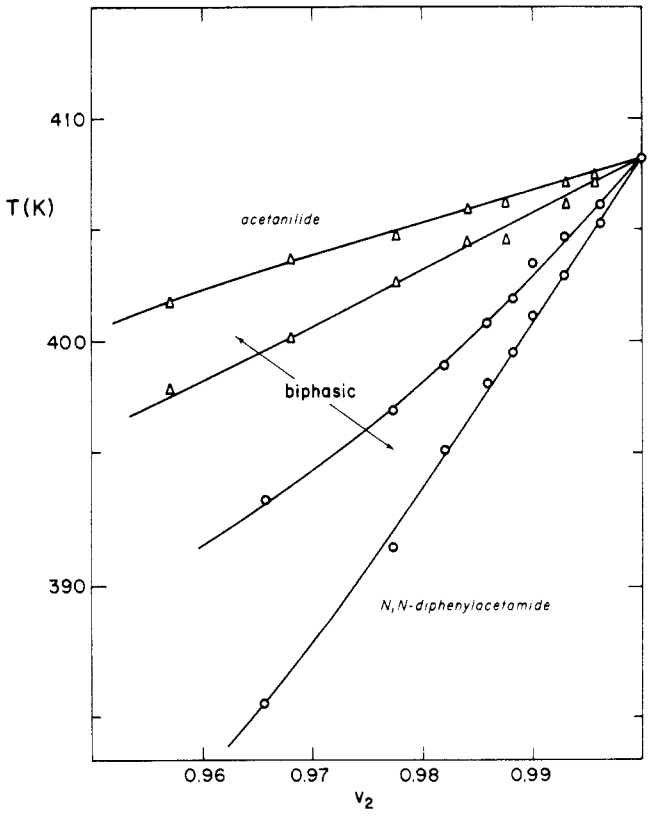

Figure 5. Comparison of the observed biphasic regions for binary systems consisting of *p*-azoxyanisole with diluents acetanilide (triangles) and *N,N*-diphenylacetamide (circles).

AA/PAA than for DPA/PAA.

The standard state selected above for the nematogenic component has the advantage that it allows treatment of the crystal–nematic transition in the usual manner. At constant temperature and pressure, the condition for equilibrium between the crystal and the binary melt is $\mu_2^K = \mu_2'$, where μ_2^K represents the chemical potential of the nematogen in the crystalline phase. Hence

$$\mu_2^K - \mu_2^{\#} = -\Delta H_{KN}(1 - T_{KN}/T_{KN}^\circ) = \mu_2' - \mu_2^{\#} \quad (14)$$

from which we obtain

$$T_{KN} = \{1 - (\zeta RT^*/\Delta H_{KN})[(v_2's - s_0) - (1/2)\{(v_2's)^2 - s_0^2\}]\}/\{(1/T_{KN}^\circ) - (R/\Delta H_{KN})[-\ln v_2' - v_1' + (\bar{y}_0 - v_2'\bar{y}) + \ln (f_1/f_1^\circ) - \zeta\chi v_1'^2]\} \quad (15)$$

Crystal–nematic transition temperatures measured at very low diluent concentrations for the DPA/PAA and AA/DPA systems appear plotted against the volume fraction of PAA in Figure 6. The full curve represents the values predicted according to eq 14 with $\zeta = 3.6$. In this case the results for the two diluents coincide, as predicted, but again the predicted depression is too large. As indicated by the dashed curve, the observed depression can be accommodated by reducing the axial ratio to 1.0, but this value would not be physically meaningful.

We intended to evaluate the χ_1 parameters by fitting the depression of the crystal–isotropic transition temperatures using the Flory–Huggins treatment. The observed melting depressions of both crystalline diluents could be fitted by using the calorimetric enthalpies of fusion, but for both systems the melting depressions of PAA could not be so represented if ΔH_{KI} were assumed to be given approximately by the sum of ΔH_{KN} and ΔH_{NI}. For example, the depression of the melting temperature of DPA could be fitted with $\Delta H_f = 5.30$ kcal/mol, which stands in reasonable agreement with the DSC value, 5.49 kcal/mol. However, fitting the K–I transitions of PAA gave ΔH_{KN} and ΔH_{NI} values determined by DSC, 6.83 kcal/mol. The existence of different crystal polymorphs of PAA intro-

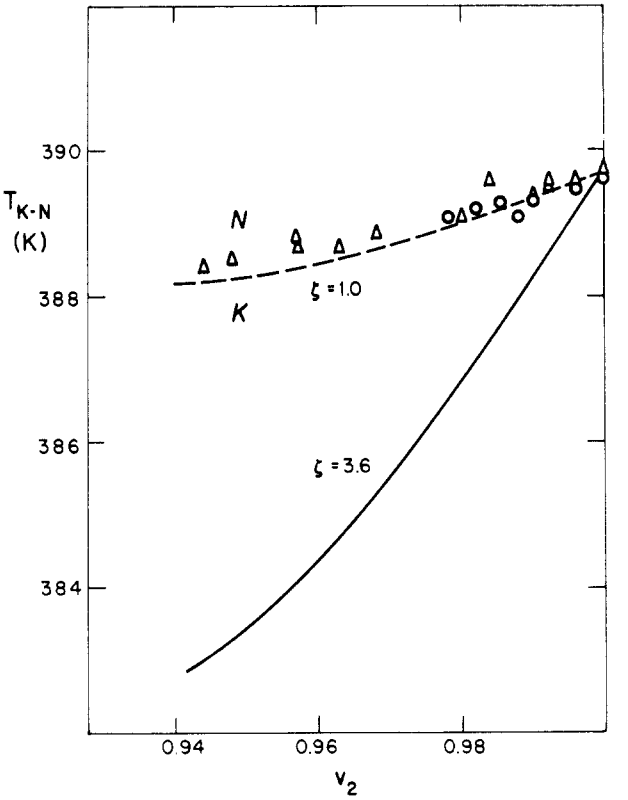

Figure 6. Crystal–nematic transition temperatures (symbols same as Figure 5) compared with the depressions predicted for axial ratios 3.6 (full curves) and 1.0 (dashed curves).

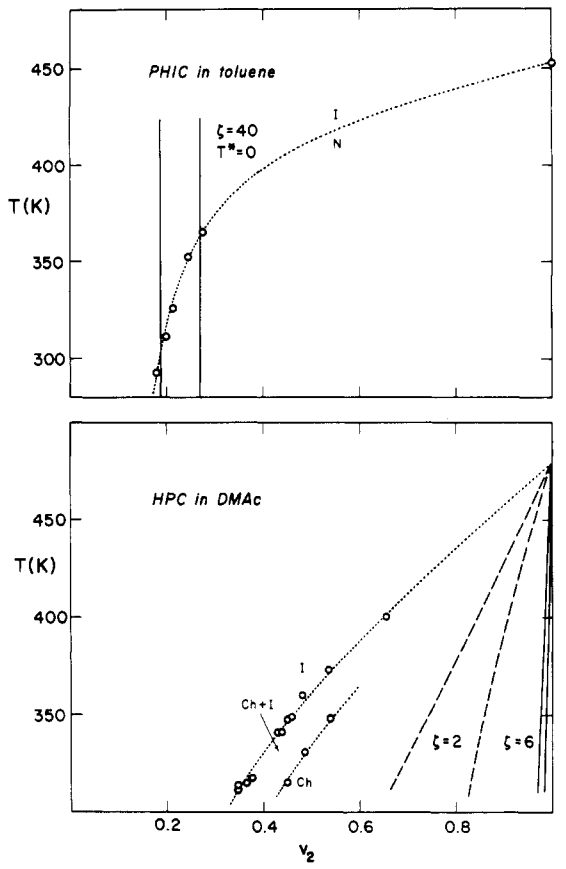

Figure 7. (Above) the variation of T_{NI} with v_2 for PHIC sample KI in toluene (dotted curve) compared with the temperature dependence of the biphasic region predicted by the Warner–Flory treatment for axial ratio 40. (Below) a similar comparison of the data of Conio et al.[40] for (hydroxypropyl)cellulose in dimethylacetamide (dotted curves) with the Warner–Flory theory for axial ratios 6 (full curves) and 2 (dashed curves).

duces some uncertainty into those transitions involving the crystalline phase.

Binary Systems Involving Polymer. As indicated in the Introduction, the theoretical treatment of polymers displaying thermotropic mesophases is in a preliminary stage. If we adopt Flory's conclusion[24] that the mesophase behavior of Kuhn chain polymers is primarily determined by the axial ratio of the Kuhn link, it should be possible to described the behavior of certain types of binary polymer–diluent systems using the treatment of Warner and Flory.[6] The only modification required is to define ζ as the axial ratio of the Kuhn link, rather than that of the molecule. For a Kuhn chain the critical axial ratio, above which only lyotropic mesomorphism is observed, is somewhat larger[24,25]—ζ_{crit} = 6.7018—as compared to the value 6.417 for rods.

The characteristics of the PHIC samples investigated are collected in Table IV. Figure 7 illustrates the temperature dependence of the critical volume fraction of PHIC in toluene. We also include the data of Conio et al.[40] for (hydroxypropyl)cellulose (HPC) in dimethylacetamide. The cholesteric phase of HPC is indicated by the symbol Ch in the figure. As previously shown, and in agreement with predictions for the Kuhn model, the critical concentration approaches an asymptotic limit with molecular weight for both PHIC[27] and HPC.[40] The data for both PHIC and HPC shown in Figure 7 do, in fact, correspond to such an asymptotic behavior. The experimental value of $T_{NI}°$ (at $v_2' = 1$) for PHIC, 453 K, is the asymptotic limit of $T_{NI}°$ at high molecular weight as illustrated in Figure 8 (cf. also Table IV). A small increase of $T_{NI}°$ with molecular weight was also reported for HPC by Seurin et al.[41] The value of $T_{NI}°$ for HPC, 480 K, appearing in Figure 7 was deduced from the latter work. The full and dashed lines represent the location of the biphasic region as calculated by the Warner–Flory treatment for various values of the axial ratio ζ. In the upper part of the figure we take ζ = 40, which is close to the experimental value for PHIC at 25 °C, and T^* = 0. In this case the bulk polymer will not exhibit a thermotropic transition, and the predicted phase diagram consists of a narrow biphasic region. In the lower portion of Figure 7 we take ζ = 6, which approximates the experimental value for HPC at $T_{NI}°$ (cf. seq.). It is immediately evident that in all cases the experimental dependence upon v_2 spans a much broader range than that predicted. Even a reduction of ζ to 2 (dashed curves in the lower diagram) gives a predicted depression of the transition temperatures which is still too large. In fact, the differences between the predicted and observed temperatures are sufficiently marked to suggest that the role of T^* is a very secondary one and some other factor must enter in a significant way.

Table IV
Characteristics of the PHIC Samples

sample[a]	$[\eta]^{25}_{toluene}$, dL/g	$\bar{M}_v$	T_{NI}, °C
AI	3.44	79 000	
AI[f]	1.48	35 300	173
AI[f]	5.55	124 500	
AI[f]	6.50	144 700	
AI[f]	7.65	169 000	
AII	5.90	131 900	
DI	4.45	100 900	175
DII	9.20	201 500	179
KI	12.9	278 000	180
KII	24.6	514 000	180

[a] f = fraction.

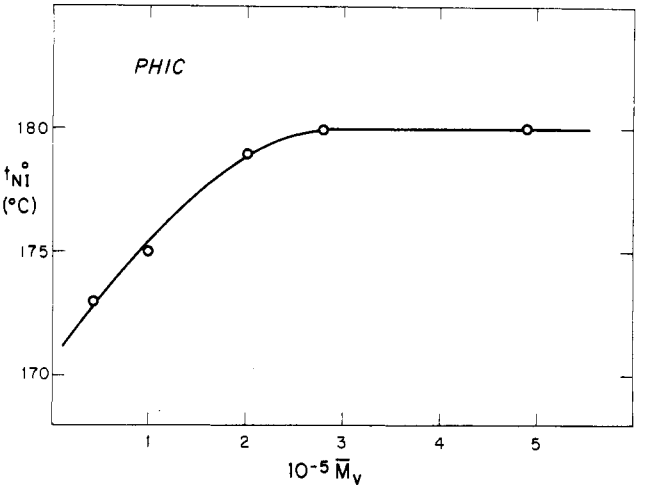

Figure 8. Variation of the nematic–isotropic transition temperature for bulk PHIC with molecular weight.

As mentioned earlier, another possible mechanism for a thermotropic transition in polymers might arise from the temperature dependence of the axial ratio of the Kuhn link. Even in the absence of orientation-dependent interactions, a transition is expected at that temperature at which the axial ratio of the Kuhn link decreases to the critical value. In treating this possibility, we will adopt the nomenclature used by Matheson and Flory[25] for chains having rodlike sequences at fixed locations, but we replace their η by ζ. Let the chain consist of γ Kuhn links, each of axial ratio ζ, so that the total number of segments in the chain is $x = \gamma\zeta$. The persistence length, q, is related to the unperturbed mean-square displacement length, $\overline{r_0^2}$,

by $2q = \overline{r_0^2}/L$, where L is the contour length of the chain. The length of a Kuhn link is given by $2q$. Thus, for a chain of diameter d, $\zeta = 2q/d$. We define the temperature coefficient, $-\xi$, by

$$\mathrm{d} \ln \zeta / \mathrm{d}T = -\xi \tag{16}$$

Hence, the temperature dependence of the axial ratio of the Kuhn link is given by

$$\zeta = \zeta_0 e^{-\xi(T-T_0)} \tag{17}$$

where the reference temperature, T_0, is taken to be the nematic–isotropic transition temperature of the polymer, $T_{NI}°$, and $\zeta_0 = \zeta_{crit}$. The value of y_0 for the nematic phase with equilibrium disorder is obtained by making $(\partial \ln Z_B/\partial y)_T$ vanish, where Z_B is the partition function[25] for the bulk nematic phase formed by the Kuhn chain polymer

$$\zeta_0 = y_0 \exp(2/y_0) \tag{18}$$

and the change in the Gibbs free energy at the nematic–isotropic transition of the bulk polymer is expressed by

$$\Delta G_{NI}° = \mu_2° - \mu_2^{\#} = xRT[(1 - y_0/\zeta) - (2/\zeta)\{\ln (\zeta/y_0) + 1\}] \tag{19}$$

Since the free energy difference vanishes at $T_{NI}°$, this yields

$$\zeta_0 = y_0 + 2 \ln (\zeta/y_0) + 2 \tag{20}$$

Application of eq 18 allows this to be written as

$$\zeta_0 = y_0 + (4/y_0) + 2 \tag{21}$$

Equations 18 and 21 can be solved simultaneously to obtain values of $\zeta_0 = \zeta_{crit}$ and y_0. From eq 19 the enthalpy change for the bulk polymer at the nematic–isotropic transition temperature is given by

$$\Delta H_{NI} = \frac{4RT_{NI}^2}{x_K y_0}\left(-\frac{\mathrm{d} \ln \zeta}{\mathrm{d}T}\right) \tag{22}$$

where x_K is the number of repeating units in the Kuhn link.

For a binary system formed by adding a spherical diluent, the analogue of eq 18 is[25]

$$\ln (v_i' + v_2' y/\zeta) = -2/y \tag{23}$$

In the nematic phase, the chemical potentials of the polymer (relative to the single-component polymeric nematic phase with equilibrium y value) and of the diluent (relative to that of the pure liquid component) are[25]

$$(\mu_2' - \mu_2^{\#})/RT = \ln v_2' - (x - 1)v_1' + x(e^{-2/y} - e^{-2/y_0}) - 2\gamma \ln (y/y_0) + x\chi v_1'^2 \tag{24}$$

$$(\mu_1' - \mu_1°)/RT = \ln v_1' + (1 - 1/x)v_2' + 2/y + e^{-2/y} - 1 + \chi_1 v_2'^2 \tag{25}$$

and the corresponding relations for the isotropic phase are

$$(\mu_2 - \mu_2^{\#})/RT = \ln v_2 - (x - 1)v_1 + x(e^{-2/y_0} - e^{-2/y}) - 2\gamma + 2\gamma \ln y_0 + x\chi_1 v_1^2 \tag{26}$$

$$(\mu_1 - \mu_1°)/RT = \ln v_1 + (1 - 1/x)v_2 + \chi_1 v_2^2 \tag{27}$$

The thermodynamic conditions for equilibrium between the binary nematic and isotropic phases are $\mu_2' = \mu_2$ and $\mu_1' = \mu_1$. The first condition produces the relation

$$\ln (v_2'/v_2) + x[\{(yv_2'/\zeta) - v_2\} - (v_2' - v_2) + 2\gamma(1 - y/\zeta) + x\chi_1(v_1'^2 - v_1^2) = 0 \tag{28}$$

while the second gives

$$\ln (v_1'/v_1) + [(y/\zeta) - (1/x)]v_2' - (1 - 1/x)v_2 + 2/y + \chi_1(v_2'^2 - v_2^2) = 0 \tag{29}$$

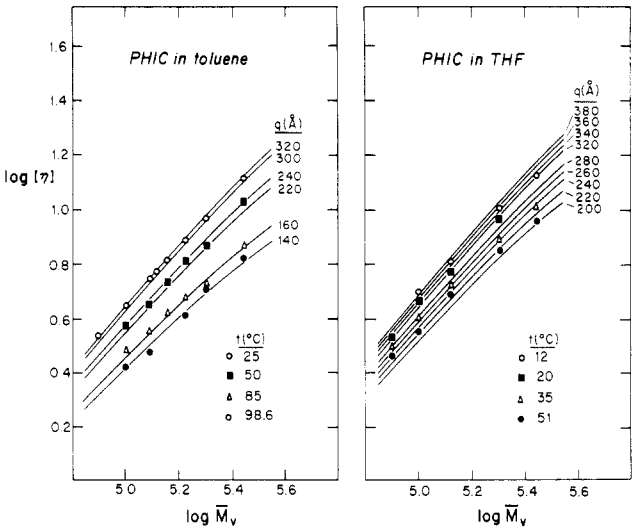

Figure 9. Full curves represent the molecular weight dependence of $[\eta]$ as calculated from the Yamakawa–Fujii treatment[42] for wormlike chains having $M_L = 63.5$, diameter 16.4 Å, and the indicated values of the persistence length q. The experimental points represent intrinsic viscosities of fractionated and unfractionated samples of PHIC in two solvents at the indicated temperatures.

Dividing the first of these relations by x and subtracting the second produces an alternative equation:

$$\frac{1}{x}\ln\left(\frac{v_2'}{v_2}\right) - \ln\left(\frac{v_1'}{v_1}\right) + \frac{2}{\zeta}\left(1 + \ln\frac{\zeta}{y}\right) - \frac{2}{y} - 2\chi_1(v_2' - v_2) = 0 \tag{30}$$

Two of the equations 28–30 must be solved simultaneously to determine v_2' and v_2. One can calculate ζ for given values of $T_{NI}°$, ξ, and T_{NI}. Since y is a function of v_2', for each T_{NI} one must iterate to obtain a self-consistent set of the parameters y, v_2' and v_2 which simultaneously satisfy two of the equations 28–30.

In order to test the validity of the above treatment, we consider the temperature dependence of the persistence length, q, for PHIC. In Figure 9 are shown theoretical curves of the molecular weight dependence of the intrinsic viscosity, $[\eta]$, calculated according to the Yamakawa–Fujii treatment[42] for selected values of q, as previously described.[27] For these calculations a value of 2 Å was taken for the residue vector[27,28] and, from examination of molecular models, the chain diameter was assigned as 16.4 Å.[27] This value is close to $d = 16$ Å reported by Murakami et al.[43] from light scattering data for PHIC in hexane. Moreover, in previous work[27] we showed tht $d = 16$ Å would secure agreement between the value of v_2' at 20 °C and that calculated from the limiting behavior of the Kuhn model. Experimental values of $[\eta]$ at various temperatures for PHIC samples in toluene and THF are superimposed on the theoretical curves. The fitted values of q, as well as those of the axial ratio, ζ, of the Kuhn link are collected for various temperatures in Table V. The variation of the axial ratio with temperature is shown in Figure 10, where $\ln \zeta$ is plotted against the reduced temperature, $T/T_{NI}°$. A similar temperature dependence of q is observed in toluene and THF. Extrapolation to a reduced temperature of unity yields an axial ratio which practically coincides with the critical value, $\zeta_{crit} = 6.7$, for the Kuhn chain polymer. Also included in Figure 10 are the data for HPC reported by Aden et al.[44] Although this extrapolation involves a larger uncertainty, the ζ value at $T_{NI}°$ for HPC appears to be somewhat lower than the critical axial ratio. This difference may indicate the presence of orientation-

Table V
Temperature Dependence of the Persistence Length of PHIC in Toluene and THF

t, °C	q, Å	ln $(2q/d)^a$	t, °C	q, Å	ln $(2q/d)^a$
A. Toluene			B. THF		
25	310	3.63	12	360	3.78
50	230	3.33	20	320	3.66
85	160	2.97	35	250	3.42
98.6	140	2.84	51	220	3.29

$^a d$ = 16.4 Å.

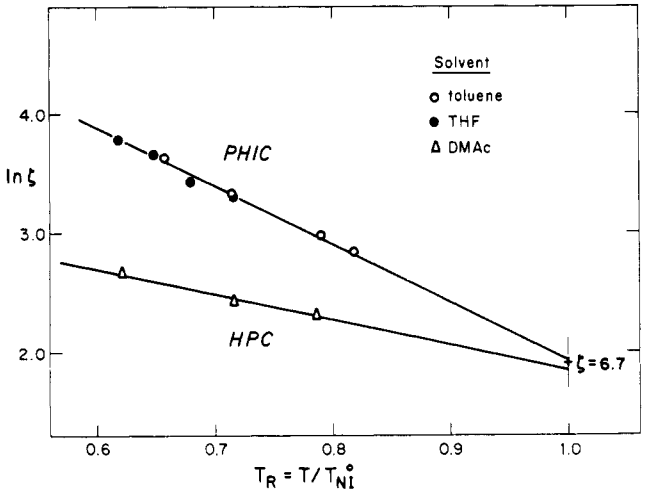

Figure 10. Temperature dependence of the axial ratio, $\zeta = 2q/d$, for PHIC in toluene and THF plotted as ln ζ vs. reduced temperature, $T_R = T/T_{NI}°$. The lower curve represents data of Ciferri and co-workers[40] for hydroxypropylcellulose in DMAc.

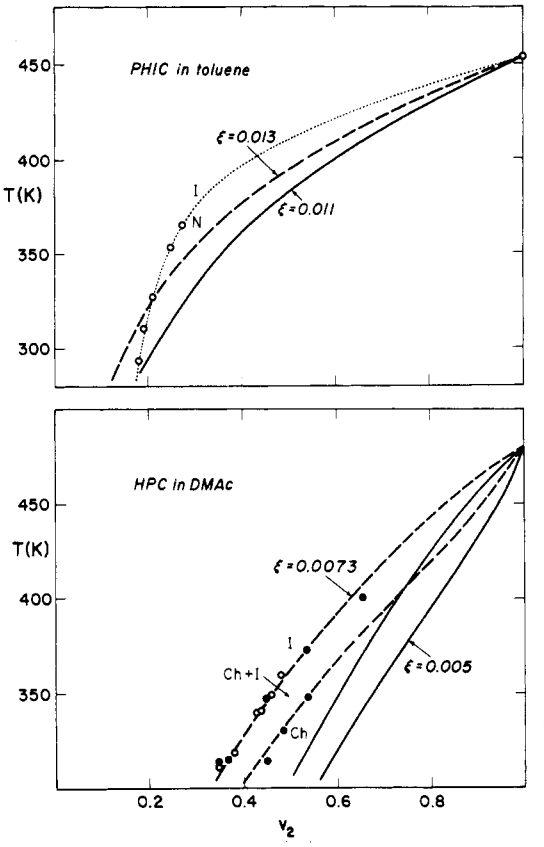

Figure 11. Comparison of the experimental behavior of PHIC in toluene and of HPC in DMAc with predictions taking into account the temperature dependence of the axial ratio. The full and dashed curves for PHIC are calculated with $\xi = -(\mathrm{d} \ln \zeta/\mathrm{d}T)$ equal to 0.011 and 0.013, respectively. The full and dashed curves for HPC represent the predicted behavior for ξ = 0.005 and 0.0073, respectively.

dependent interactions. As discussed elsewhere,[44] a T^* value of about 150 K would secure agreement with both the isothermal and thermotropic behavior of HPC. However, since the Flory treatment of the Kuhn chain polymers does not predict values for the order parameter, orientation-dependent interactions cannot be included in that treatment. In the case of PHIC, the long aliphatic side chain makes it unlikely that soft interactions stabilize the mesophase to any significant extent, so the result obtained in Figure 10 is in line with the expectation that $T^* = 0$ for this polymer.

A more detailed test of the above treatment is illustrated in Figure 11. From the slopes in Figure 10, the values of $\mathrm{d}(\ln \zeta)/\mathrm{d}T$ are found to be −0.011 and −0.005 for HPC and PHIC, respectively. The full curves in Figure 11 indicate the variation of v_2 with temperature for these two polymers calculated by using the above values. The predicted depressions are again too strong, although the agreement between theory and experiment is significantly better than that obtained by using the Warner–Flory treatment (cf. Figure 7). For HPC, agreement between experiment and the Kuhn model with $T^* = 0$ is obtained upon increasing ξ from 0.05 to 0.073. The latter is close to the value reported by Brandt and Goebel[45] for cellulose derivatives. Upon inserting the experimental values of ξ into eq 22 we obtain ΔH_{NI} = 300 and 500 cal/(mol of repeating unit) for PHIC and HPC, respectively.

Some features of our data for PHIC deserve comment. We note that $\mathrm{d}(\ln \zeta)/\mathrm{d}T$ for PHIC is quite large in absolute magnitude. Several earlier workers[28,46,47] have observed that $[\eta]$ for PHIC in various solvents decreases strongly with increasing temperature. This is not surprising and reflects the altering hydrodynamic character as the molecule changes from a rodlike to a coiling conformation with increasing temperature. Our data, in common with those of Pierre and Desreux[46] for PHIC in CCl_4, indicate that the absolute magnitude of $\mathrm{d} \ln [\eta]/\mathrm{d}T$ increases with molecular weight. Moreover, even for the highest molecular weight, the latter derivative is smaller than the magnitude of $\mathrm{d}(\ln \zeta)/\mathrm{d}T$. Coles et al.[48] have reported evidence for aggregation of PHIC in toluene. This might offer an explanation for the two unusual features just cited, and for the difference between the experimental and theoretical curves appearing in Figure 11 in the low temperature range. On the other hand, the temperature dependence of the persistence length of PHIC is nearly the same in toluene and THF, and we are not aware of any evidence in the literature suggesting aggregation of PHIC in the latter solvent.[28]

Concluding Remarks

We have determined the phase diagrams for two binary systems involving the low molecular weight nematogen *p*-azoxyanisole (PAA) to provide a test of the Warner–Flory treatment. Theory predicts that the transition temperatures of the biphasic region should be the same for all diluents. We find, instead, that the biphasic temperatures are depressed to a lesser extent by acetanilide (AA) than by *N*,*N*-diphenylacetamide (DPA). When the data for these two systems are fitted to eq 1, the resulting ΔS_{NI} values are 1.87 cal/(mol K) for AA/PAA and 0.42 cal/(mol K) for DPA/AA. The latter is in reasonable agreement with the value 0.39 cal/(mol K) measured by DSC (Table I), but the former is almost 5 times as large. Differences in the shapes of the diluent molecules may offer one explanation for these observations. Martire are co-workers[14,15] investigated the effect of different diluents

upon several low molecular weight nematogens. They observed that normal hydrocarbons give smaller depressions than pseudospherical molecules and, among the latter, those having larger molecular diameters give larger depressions. For different tetraalkyltin diluents with (4-methoxybenzylidene)-4-butylaniline (MBBA) they reported slopes which ranged over a factor of about 2.5, and apparent ΔS_{NI} values which varied by a factor of 5. It seems quite reasonable that a rodlike molecule which is not quite nematogenic (having a virtual T_{NI}) should disrupt the structure of the nematic phase much less than a large spherical diluent. The Warner–Flory treatment cannot account for possible effects of different diluent shapes since it considers only small spherical diluents that occupy a single lattice site. Hydrogen bonding may offer another explanation of the observations for the systems considered here. We note that the two diluents give different slopes in the limit as the volume fraction of diluent vanishes. This could only be explained if the hydrogen bonding occurred between the two species, AA and PAA. Of course, this type of hydrogen bonding is not possible with DPA. If PAA is assigned the axial ratio 3.6, as deduced by Flory and Ronca from crystallographic data, the predicted depressions of the biphasic transition temperatures are too large. Also, theory requires the orientation-dependent interactions to be too strong, resulting in a predicted ΔH_{NI} which is nearly 6 times the experimental value. The two binary systems show nearly the same depression of the crystal–nematic transition temperature, as expected from theory; however, the predicted depression is also too large for this transition.

Turning to polymeric nematogens, extrapolation of the axial ratio of the Kuhn link for PHIC to $T_{NI}°$ produces a value very close to the critical axial ratio for a Kuhn chain polymer. Thus, orientation-dependent interactions may not be necessary to stabilize the nematic phase of this polymer. Predictions based upon this supposition, using experimental values of ξ, produce depressions of the biphasic temperatures with diluent concentration which are in better agreement with experiment than those obtained by using the Warner–Flory treatment. A significant feature of this treatment is the prediction that all polymers which can be described by the Kuhn chain model with temperature-dependent dimensions should be in corresponding states at their nematic–isotropic transition temperatures. We expect that a variety of polymers can be represented as a Kuhn chain with temperature-dependent dimensions. This suggests that even those polymers normally classified as having rigid chains, such as the para-linked aromatic polyesters, may have large negative ξ values, casting doubt upon the expectation that $T_{NI}°$ will be infinite for this class of polymers.

Our observations for semiflexible polymers suggest that the variation of the unperturbed dimensions with temperature plays an essential role in thermotropic mesophase behavior of polymers. Indeed, it seems unlikely that thermotropic polymer systems can be treated successfully without taking this variation into account. While the effect of temperature upon the unperturbed dimensions of polymers has been fairly well characterized, the effect of temperature upon the average conformation of small molecules is less well explored. It seems quite possible that the population of conformers of many of the small molecule mesogens may be temperature dependent and that this variation could affect the mesophase properties. On the other hand, a more refined treatment of semiflexible polymers should simultaneously consider the effects of $d(\ln \zeta)/dT$ and T^* upon T_{NI}.

Newer treatments are being developed which include some of the effects mentioned above. Seurin et al.[41] analyzed data for HPC in terms of their treatment[49] involving a threadlike molecule having a bending force constant, and including Maier–Saupe interactions in the mean-field approximation. According to this theory, there is no critical axial ratio (or persistence length) above which a thermotropic nematic–isotropic transition is impossible. If the bending constant is assumed to be independent of temperature, the persistence length of the chain must be temperature dependent. They deduce an interchain interaction energy of about 0.4 kcal/mol for HPC, which is in reasonable agreement with $T^* = 150$ K.[44] However, they do not indicate the magnitude of dq/dT predicted or measured for this polymer. These workers attribute the increase of $T_{NI}°$ with polymer molecular weight observed for HPC[41] and poly(*n*-nonyl isocyanate)[50] to quadrupolar interactions. This differs from our conclusion that $T^* = 0$ for PHIC. We attribute the molecular weight dependence of $T_{NI}°$ shown for PHIC in Figure 8 to the transition from rodlike to coiling behavior. Ronca and Yoon[51] also treat a threadlike model chain with a bending force constant but, unlike the treatment of ten Bosh et al.,[49] these workers include in their partition function a factor for the number of degrees of conformational freedom accessible to a system of chains subjected to overall conformational constraints. In the long chain limit, their limiting axial ratio is 6.68, which is practically identical with the limit, 6.70, used here. Their predicted dependence of $T_{NI}°$ upon molecular weight for small values of q/d (appropriate for PHIC at about 180 °C) is qualitatively in agreement with our observations for PHIC. Their treatment should be particularly useful in predicting the trends with molecular weight as the long chain limit is approached. However, thus far they have not incorporated orientation-dependent interactions into their theory.

Acknowledgment. This work was supported by the National Science Foundation Division of Materials Research and the Industry-University Cooperative Research Program through grant DMR-81-06160 and by the Italian C.N.R.

References and Notes

(1) Onsager, L. *Ann. N.Y. Acad. Sci.* **1949**, *51*, 627.
(2) Ishihara, A. *J. Chem. Phys.* **1950**, *18*, 1446; **1951**, *19*, 1142.
(3) Flory, P. J. *Proc. R. Soc. London, Ser. A* **1956**, *234*, 73.
(4) Maier, W.; Saupe, A. *Z. Naturforsch.* **1959**, *149*, 882; **1960**, *159*, 187.
(5) Flory, P. J.; Ronca, G. *Mol. Cryst. Liq. Cryst.* **1979**, *54*, 311.
(6) Warner, M.; Flory, P. J. *J. Chem. Phys.* **1980**, *73*, 6327.
(7) Smith, G. W. *Mol. Cryst. Liq. Cryst.* **1979**, *49*, 207.
(8) Lewis, I. C.; Kovac, C. A. *Mol. Cryst. Liq. Cryst.* **1979**, *51*, 173.
(9) Lewis, I. C.; Barr, J. B. *Mol. Cryst. Liq. Cryst.* **1981**, *72*, 65.
(10) Irvine, P. A.; Wu, DaChang; Flory, P. J. *J. Chem. Soc., Faraday Trans. 1* **1984**, *80*, 1795.
(11) Krigbaum, W. R.; Ciferri, A. *J. Polym. Soc., Polym. Lett. Ed.* **1980**, *18*, 253.
(12) de Kock, A. C. *Z. Phys. Chem.* **1904**, *48*, 129.
(13) Rothmund, V. *Z. Phys. Chem.* **1897**, *24*, 705.
(14) Martire, D. E.; Oweimreen, G. A.; Aigren, G. I.; Ryan, S. G.; Peterson, H. T. *J. Chem. Phys.* **1976**, *64*, 1456.
(15) Martire, D. E. In "The Molecular Physics of Liquid Crystals"; Luckhurst, G. R., Gray, G. W., Eds.; Academic Press: New York, 1979; Chapter 10.
(16) Kronberg, B.; Patterson, D. *J. Chem. Soc., Faraday Trans. 2* **1976**, *721*, 1686.
(17) Flory, P. J. *Proc. R. Soc. London, Ser. A* **1956**, *234*, 60.
(18) Cox, R. J.; Johnson, J. F. *IBM J. Res. Dev.* **1978**, *22*, 51.
(19) Peterson, H. T.; Martire, D. E.; Cotter, M. A. *J. Chem. Phys.* **1974**, *61*, 3547.
(20) Agren, G. I.; Martire, D. E. *J. Phys. C* **1975**, *36*, 141.
(21) Dowell, F.; Martire, D. E. *J. Chem. Phys.* **1978**, *68*, 1094; **1978**, *69*, 2332.
(22) Dowell, F. *J. Chem. Phys.* **1978**, *69*, 4012.

(23) DiMarzio, E. A. *J. Chem. Phys.* **1961**, *35*, 658.
(24) Flory, P. J. *Macromolecules* **1978**, *11*, 1141.
(25) Matheson, R. R.; Flory, P. J. *Macromolecules* **1981**, *14*, 954.
(26) See, for example: Flory, P. J. "Statistical Mechanics of Chain Molecules"; Interscience: New York, 1969; p 39.
(27) Conio, G.; Bianchi, E.; Ciferri, A.; Krigbaum, W. R. *Macromolecules* **1984**, *17*, 856.
(28) Berger, M. N.; Tidswell, B. M. *J. Polym. Sci., Polym. Symp.* **1973**, *42*, 1603.
(29) Aharoni, S. M.; Walsh, E. K. *Macromolecules* **1979**, *12*, 271.
(30) Bernal, J. D.; Crowfoot, D. *Trans. Faraday Soc.* **1933**, *29*, 1032.
(31) Robinder, R. C.; Poirier, J. C. *J. Am. Chem. Soc.* **1968**, *90*, 4760.
(32) Arnold, H. *Z. Phys. Chem.* **1964**, *226*, 148.
(33) Barrall, E. M.; Porter, R. S.; Johnson, J. F. *J. Phys. Chem.* **1967**, *71*, 895.
(34) Chou, L. C.; Martire, D. E. *J. Phys. Chem.* **1969**, *73*, 1127.
(35) Neumann, A. W.; Kimentowski, L. J. *J. Therm. Anal.* **1974**, *6*, 67.
(36) Neumann, A. W.; Springer, R. W.; Bruce, R. T. *Mol. Cryst. Liq. Cryst.* **1974**, *27*, 23.
(37) Bata, L.; Broude, L.; Federov, V. G.; Kiriv, N.; Rosta, L.; Stabon, J.; Umarov, L. M.; Vizi, I. *Mol. Cryst. Liq. Cryst.* **1978**, *44*, 71.
(38) Ogorodnik, K. Z.; Karazhaev, V. D. *Sov. Phys.—Crystallogr. (Engl. Transl.)* **1981**, *26*, 486.
(39) Flory, P. J.; Irvine, P. A. *J. Chem. Soc., Faraday Trans. 1* **1984**, *80*, 1807.
(40) Conio, G.; Bianchi, E.; Ciferri, A.; Tealdi, A.; Aden, M. A. *Macromolecules* **1983**, *16*, 1264.
(41) Seurin, M. J.; ten Bosch, A.; Sixou, P. *Polym. Bull.* **1983**, *9*, 450.
(42) Yamakawa, H.; Fujii, M. *Macrmolecules* **1974**, *7*, 128.
(43) Murakami, H.; Norisuye, T.; Fujita, H. *Macrmolecules* **1980**, *13*, 345.
(44) Aden, M. A.; Bianchi, E.; Ciferri, A.; Conio, A.; Tealdi, A. *Macromolecules*, in press.
(45) Brandt, D. A.; Goebel, K. D. *Macromolecules* **1972**, *5*, 536.
(46) Pierre, J.; Desreux, V. *Polymer* **1974**, *15*, 685.
(47) Anderson, J. S.; Vaughan, W. E. *Macromolecules* **1975**, *4*, 454.
(48) Coles, H. C.; Gupta, A. K.; Marchal, E. *Macromolecules* **1977**, *10*, 182.
(49) ten Bosh, A.; Maissa, P.; Sixous, P. *J. Phys., Lett.* **1983**, *44*, L105; *J. Chem. Phys.* **1983**, *79*, 3462.
(50) Seurin, M. J.; ten Bosh, A.; Sixou, P. *Polym. Bull.* **1983**, *10*, 434.
(51) Ronca, G.; Yoon, D. Y. *J. Chem. Phys.* **1982**, *76*, 3295; **1984**, *80*, 925, 930.

Critical Exponents for Off-Lattice Gelation of Polymer Chains

L. Y. Shy, Y. K. Leung, and B. E. Eichinger*

Department of Chemistry, BG-10, University of Washington, Seattle, Washington 98195.
Received July 30, 1984

ABSTRACT: The random polycondensation of telechelic linear chains cured with tri- and tetrafunctional cross-linkers has been simulated. Calculations are done for both bulk and solution reactions; critical points are located by different methods, with results in good agreement with experiment. Critical exponents β and γ vary from system to system, with average values $\beta = 0.300 \pm 0.024$ and $\gamma = 1.77 \pm 0.16$. The average value $C_-/C_+ = 13.58 \pm 3.50$ is slightly larger than that from standard percolation.

The statement[1] that "random gelation is nothing but bond percolation on a continuum" characterizes efforts[2-5] to determine the universality class for gelation. Most of the simulations have been done on lattices, which leaves unanswered several questions related to the influence of underlying order on an inherently disordered phenomenon. Continuum percolation of noninteracting disks[6] in two dimensions appears to be in the same universality class as lattice percolation, but this is not a realistic physical model for polymer gelation.

In our model, prepolymer chains and cross-linkers are randomly distributed in a cubical box. Simulations (not described here) show that intermolecular correlations are relatively unimportant for polymer gelation if the chain concentration is above about 30% by weight. (Equilibrium correlations are short-range, but gelation is primarily dependent on long-range correlations. Furthermore, the transition-state intermediates that inevitably accompany bond formation are not at thermodynamic equilibrium.) One end of each chain is located with uniformly distributed random numbers, and the other end has a Gaussian distribution with one-dimensional variance given[7] by $\sigma^2 = C_n n l^2/3$. Here n is the number of skeletal bonds in the prepolymer, l is the length of one bond, and C_n is the characteristic ratio.[8] The details of the model and program have been described in previous work.[9,10] In this paper, the influence of cyclization on the critical point is investigated by varying the concentration and molecular weight of the prepolymers. The purpose is twofold: (1) to examine the model near the critical region, where some experimental data are available for comparison, and (2) to estimate critical exponents for realistic off-lattice simulations.

Table I
Estimates of Critical Extent of Reaction

system	mol wt	concn, vol %	P_c^a	P_c^b	P_c^c	η^d
		$A_2 + B_4$				
1	1850	100	0.583	0.590	0.591	5.20
2	1850	62	0.603	0.613	0.614	6.74
3	1850	26	0.652	0.661	0.658	12.22
4	11600[e]	100	0.573	0.578	0.576	2.85
5	11600	100	0.560	0.574	0.575	2.18
6	18500	100	0.556	0.568	0.569	1.92
		$A_2 + B_3$				
7	1850	100	0.700	0.718	0.712	4.15
8	11600[e]	100	0.684	0.710	0.706	3.85

[a] From DP_w extrapolation. [b] From upper–lower bound. [c] From scaling equation. [d] Percentage of intramolecular reactions at P_c^b. [e] Log-normal distribution.

The systems investigated are described chemically as $A_2 + B_i$, where A_2 is a telechelic prepolymer, and B_i ($i = 3$, 4) is a low molecular weight cross-linker with functionality equal to i. A and B groups are in equal numbers; 10 000 A_2 molecules are generated for each configuration, and results are averages of at least four configurations for each set of parameters. Bond formation between A and B groups in static configurations is controlled by varying a capture radius centered on the randomly distributed cross-linkers. Ends that fall outside the capture sphere

0024-9297/85/2218-0983$01.50/0